Proceedings of the ASME 2010 3rd Joint US-European Fluids Engineering Summer Meeting and 8th International Conference on Nanochannels, Microchannels, and Minichannels
FEDSM-ICNMM2010
August 1-5, 2010, Montreal, Canada

FEDSM-ICNMM2010-30713

A NUMERICAL 3-D MODEL OF A TRAPEZOIDAL THREE-HOLE PNEUMATIC PRESSURE PROBE FOR INCOMPRESSIBLE FLOW

Argüelles Díaz, Katia María **Fernández Oro, Jesús Manuel**
Blanco Marigorta, Eduardo **Barrio Perotti, Raúl**

Fluid Mechanics Group. University of Oviedo.
Campus de Viesques, 33271. Gijón (Asturias), Spain.
arguelleskatia@uniovi.es

ABSTRACT

Pneumatic pressure probes are well-mature measuring devices to characterize both pressure and velocity fields for external and internal flows. The measuring range of a particular probe is significantly influenced by important factors, like its geometry, the separation angle between the holes, the holes tapping or even flow conditions like separation and stagnation points or the local Reynolds number.

Ideally, every pressure probe must be specifically designed for the particular application where it is needed. However, this procedure requires a detailed calibration of the probe for the whole expected range of velocities and incidences. This implies an important cost in both economic terms and operating times. Thus, the definition of an accurate numerical model for the design and calibration of pressure probes at different flow conditions is particularly desirable for these purposes.

The first step towards the establishment of this useful methodology is the development of a reliable model to predict numerically the probe measuring characteristics. Thus, in this paper a numerical 3-D model is presented to characterize the calibration of a three-hole pneumatic pressure probe. In particular, a trapezoidal geometry with a 60 degree angle between the holes is considered here. The simulation of the flow incidence is carried out using the commercial code FLUENT, analyzing the influence of different mesh densities and turbulence models. The complete set of numerical cases includes different flow velocities and several yaw angles. The numerical results have been validated using experimental results obtained in a calibration facility, focusing on the definition of a numerical tool for the design and calibration of three-hole pneumatic probes under incompressible flow conditions.

INTRODUCTION

Pressure probes are employed to obtain pressure and velocity fields for both external and internal flows [1]. These devices are built with several holes on the probe head, where the pressure is sensed to retrieve the flow conditions afterwards. In the case of two-dimensional flows, three holes are usually sufficient to characterize the basic fluid dynamic structures. If the flow presents a clear three-dimensionality, then four holes will be at least needed to capture the complex flow features. Additionally, the probes can be designed with a great variety of head geometries (spherical, cylindrical, conical, cobra-type, etc) providing very different operational (measuring) ranges [2].

Another basic classification divides the operation of the probes into nulling [3-4] and non-nulling [5-6] modes. In the first case, the probe must be aligned with the flow direction, so the lateral holes sense identical pressure values. This is equivalent to set the incidence angle of the central hole to zero. Since this alignment must be repeated for all the measuring locations, the acquiring times are notably enlarged, reducing the practical usefulness of this system. Moreover, unsteady flows cannot be described using nulling routines, even though the pressure sensors would be of the fast-response type like Kulites or similar piezoelectric transducers. Alternatively, the non-nulling mode operates the pressure probe in a fixed position respect to the incident flow, retrieving the pressure and velocity values from a previous calibration using a data reduction technique. With this system, the acquiring times are significantly reduced, allowing the determination of full

unsteady flows when high-frequency sensors are introduced within the holes [6-7]. Consequently, pending on the technical characteristics of the sensors, pressure probes operated in the non-nulling mode can be classified into fast-response (or dynamic) and slow-response (or pneumatic) probes.

The non-nulling mode requires the definition of unique relationships between the flow angle and the velocity, the static pressure and the pressure values sensed in the holes. Such relationships are obtained through the direct calibration of the probe. Typical angular ranges of Three-Hole Pressure probes (THP probes) operating in non-nulling mode for two-dimensional flows are ± 30 deg [1]. However, it is known that this limit is not really a physical restriction of the probes, but a consequence of the mathematical procedure employed in the data reduction of traditional calibrations. The traditional calibration coefficients introduced for THP probes are:

$$C_\alpha(\alpha) = \frac{P_2 - P_3}{P_1 - 0.5(P_2 + P_3)}$$
$$C_{P_0}(\alpha) = \frac{P_0 - P_1}{P_1 - 0.5(P_2 + P_3)}; \quad C_{P_S}(\alpha) = \frac{P_0 - P_S}{P_1 - 0.5(P_2 + P_3)} \tag{1}$$

where P_1, P_2, P_3 represent the pressure values of the holes, P_0 and P_s are both total and static pressures, α is the yaw angle of the flow, and C_α, C_{P0} and C_{Ps} are the angular coefficient, the total pressure coefficient and the static pressure coefficient respectively. Note that all the calibration coefficients defined in (1) are only a function of the flow angle and fully independent of the velocity magnitude. Unfortunately, these coefficients present a singularity around +37 deg and -37 deg, leading to an apparent unavoidable reduction of the operative range of the probe to ± 30 deg.

Recent investigations of the authors [10-13] have revealed that singular points arising in (1) are not an unavoidable limitation of the angular range for THP probes. They can be suppressed discriminating a number of zones across the whole angular range for the flow where different no-singular calibration coefficients are defined. This calibration procedure is known as zone-based method. As a consequence, the angular range can be extended until a real physical limitation arises, that is, double points for the calibration coefficients or repeated zones. In the same fashion as the traditional coefficients, the new coefficients of the zone-based method depend exclusively on the flow angle, being unaffected by the velocity magnitude.

Typically, a calibration method with just two different zones is enough to provide a significant increment of the angular range (± 70 deg). For instance:

$$C_\alpha(\alpha) = \frac{P_2 - P_3}{P_1 + P_2 - 2P_3}$$
$$C_{P_0}(\alpha) = \frac{P_0 - P_1}{P_1 + P_2 - 2P_3}; \quad C_{P_S}(\alpha) = \frac{P_0 - P_S}{P_1 + P_2 - 2P_3} \tag{2}$$

where $P_2 > P_3$, and:

$$C_\alpha(\alpha) = \frac{P_2 - P_3}{P_1 + P_3 - 2P_2}$$
$$C_{P_0}(\alpha) = \frac{P_0 - P_1}{P_1 + P_3 - 2P_2}; \quad C_{P_S}(\alpha) = \frac{P_0 - P_S}{P_1 + P_3 - 2P_2} \tag{3}$$

where $P_3 > P_2$.

Not only has the calibration method an influence on the probe angular range. Other important factors, like its geometry, the separation angle of the holes and its shape, the development of detached conditions around the probe or the variation of the Reynolds number determine the operative measuring range. This means that every pressure probe should be specifically designed for the particular application where it is needed, trying to maximize the measuring range according to the specific flow conditions. Therefore, a tentative design with a fixed geometry should be tested for the flow to be measured, firstly calibrating the probe for the whole expected angular range and finally reducing the retrieved data to check if the probe is optimal. If it is not the case, then a redesign is mandatory, modifying the major geometrical features and repeating the complete validation process. Obviously, this implies a very important cost, both in economic terms and operating times. As a consequence, the definition of an accurate numerical model for the design and calibration of the probe, based on the simulation of the flow conditions around the probe head, is of particular interest for probe developers, in order to reduce the number of real tests and prototypes. The requirement is that the numerical model must predict accurately the characteristics of the probe measurements.

In essence, the objective of the present investigation is the development of a numerical model to be exploited in the design of pressure probes for specific conditions. For that purpose, a THP probe with trapezoidal head geometry and 60 deg separation angle between the holes has been built and experimentally characterized in a calibration facility. Complementarily, using the commercial code FLUENT, a numerical model of this geometry has been implemented and numerically resolved. A comparison of the numerical results and the experimental data has allowed the validation of the proposed methodology. In addition, the influence of the mesh density in the CFD computations for the numerical results as well as the selection of the turbulence model has been also explored for this paper. Moreover, the effect of the variation in the flow incidence and the Reynolds number was also considered in order to establish a feasible virtual tool for the design of THP probes. Following, the probe geometry and the experimental devices used for the calibration are described in detail. The numerical model predicting the fluid dynamic behavior of the probe is also presented. Finally, its results are discussed and validated comparing the numerical predictions with the experimental data.

PROBE GEOMETRY AND EXPERIMENTAL SETUP

A trapezoidal three-hole pneumatic pressure probe with a 60 deg construction angle (angle between its frontal faces) has been built. Figure 1 shows a sketch with the main geometrical parameters of the probe. This probe presents sharp edges where the flow can be easily detached [14].

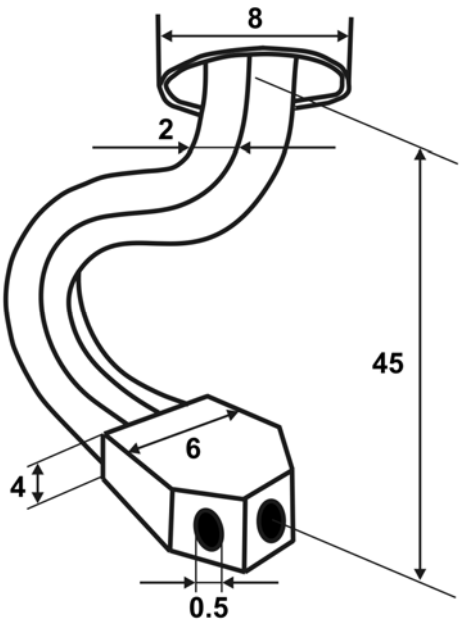

Figure 1. Three-hole trapezoidal probe. 60 deg construction angle.

The trapezoidal probe has been built mechanizing all the faces (frontal and lateral) from a raw, solid piece of aluminium. Its frontal section was fixed to 6 x 4 mm^2. Following, three small holes (compared to the total area of the faces) of 0.5 mm diameter have been drilled on the faces.

The probe is connected to the pressure transducers through intermediate pneumatic tubings of 2 m length and 4 mm of internal diameter. The transducers employed in the calibration facility are Validyne DP15, with a 350 mm H_2O measurement range and an overall precision of ±0.25%. Output data from these transducers, after amplification, are acquired with a PCI 12 bits A/D card.

The calibration facility is a small wind tunnel, operated with a centrifugal fan installed at the inlet. A settling chamber and a 4:1 contraction nozzle are placed upstream of the test section to ensure a uniform incident flow over the probe. The test section is an opened working area of 0.15 x 0.30 m^2, where the static pressure is thus atmospheric. Maximum velocity magnitude in the facility is 65 m/s, with a turbulence level around 0.5%. The velocity magnitude is determined with a Pitot-static probe measuring in the test section, and also referred to the pressure established in the settling chamber. Both measurements are monitored with pressure transducers and checked with U-manometers. The uncertainty for the mean velocity is estimated to be lower than 0.2%. The probe is held in a rotating support and driven by two step motors, so it can be axially and radially rotated 360 deg with a precision higher than 0.1 deg in both directions. A sampling frequency of 1 kHz per channel was employed for all the measurement sets. It is considered that this selection is enough accurate for pneumatic probes with slow frequency response. Also, several filters are introduced, in both the electronic hardware and the digital processing of the signals, to avoid aliasing and to filter out disturbance frequencies.

NUMERICAL MODEL

The commercial code FLUENT v6.3 has been employed to resolve the three-dimensional set of the Navier-Stokes equations assuming incompressible viscous flow. The volume finite method, expressed within a collocated grid, is combined with a first order, explicit scheme for the temporal discretization. The pressure and velocity coupling has been resolved using a SIMPLE algorithm, and both diffusive and convective terms have been implemented using a central differencing scheme.

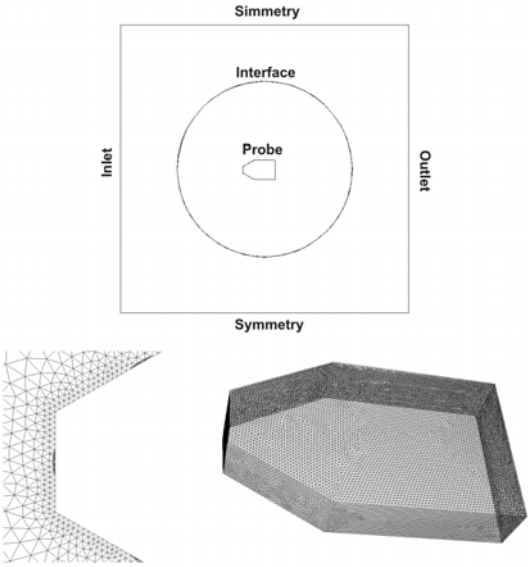

Figure 2. Geometry of the computational domain and mesh details.

A compatible pre-processor, Gambit v2.4, has been used to define the probe geometry and the mesh density of the simulations. Figure 2 shows the trapezoidal geometry for a meridional plane of the three-dimensional probe. At the inlet boundary, the flow velocity magnitude is fixed as a kinematic boundary condition, aligned with the central hole (frontal face) of the probe, thus assuming a zero incidence flow angle. At the

outlet, a constant (atmospheric) pressure value is imposed, while for the rest external limits (far away from the probe) a frictionless wall condition was selected to provide the most accurate and realistic boundary conditions. The internal complexity of the probe (internal tubings) was obviated in the model, so the parametric definition of the model could be notably simplified. Hence, the mesh generation is clearly enhanced and the computational cost efficiently controlled.

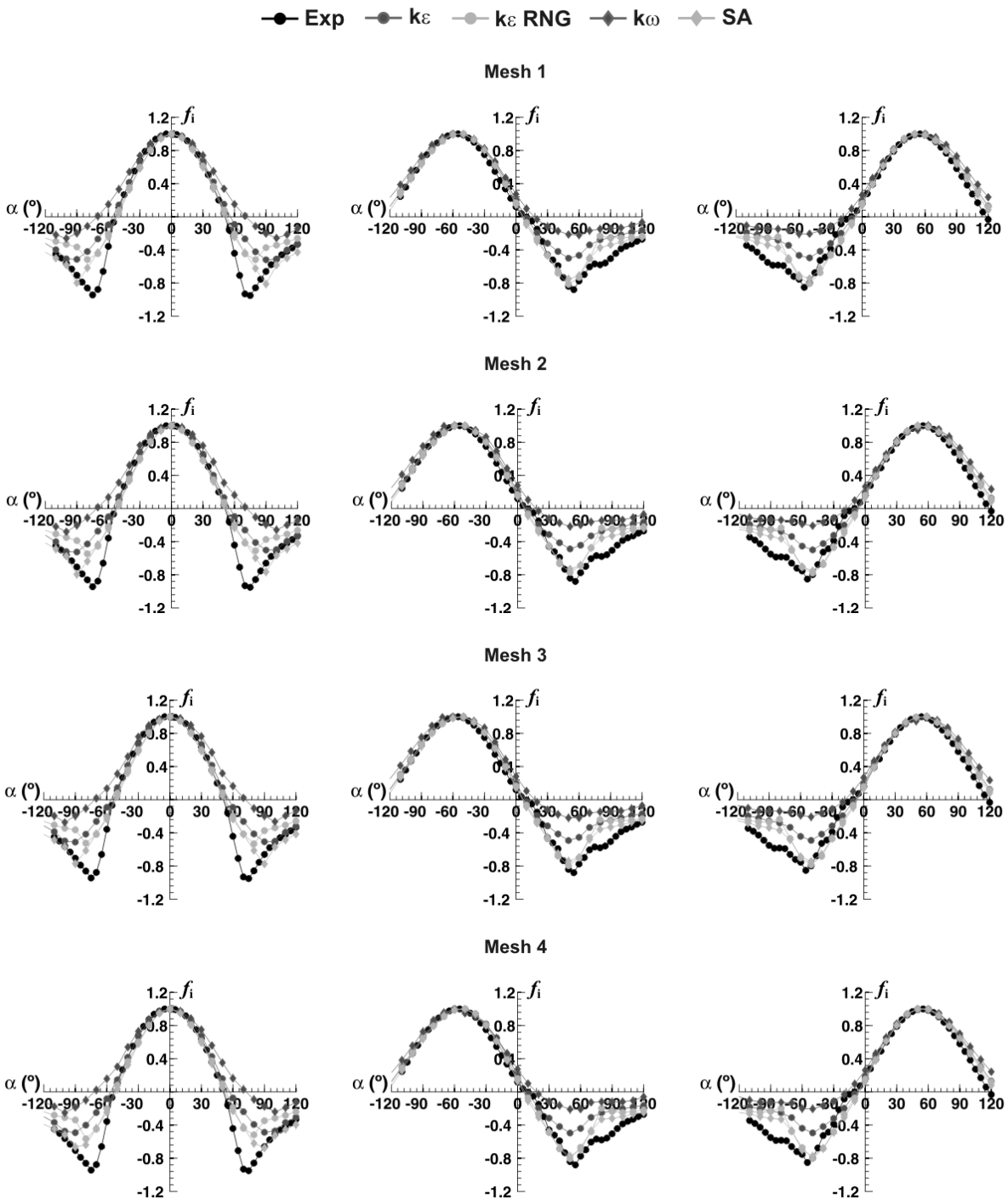

Figure 3. Numerical results obtained for the different meshes and turbulence models.

A systematic numerical calibration of the probe was achieved using a sliding mesh technique. With this approach, the probe head is rotated 2.5 deg for every time step, so it is possible to complete the whole angular calibration of the probe without defining a singular case for every flow incidence to be modelled. Notice that in this application the temporal resolution is not relevant at all, because the unsteady technique is employed exclusively to modify the incidence flow angle. Thus, the temporal time step can be made arbitrarily large; in particular, it was fixed to 1 second. To fulfil convergence, it was assured that a sufficient number of iterations were always completed for every yaw angle to meet the convergence criteria (numerical residuals for all the equations reaching 10^{-7}).

A sensibility analysis for the mesh density was conducted to establish the best option for the spatial discretization. In this investigation, four different unstructured meshes have been tested (their basic characteristics are summarized in table 1) to determine the optimal ratio between accuracy and computational cost. For convenience, the mesh density has been significantly increased close to the probe surfaces: a detail of the mesh in the proximity of the probe can be observed in figure 2.

	Nº cells	y+	Δx (mm)	Δy (mm)	Δz (mm)
M1	594.984	8.5	0.1	0.1	0.1
M2	867.020	7.9	0.08	0.08	0.08
M3	1.549.776	7.1	0.06	0.06	0.06
M4	678.523	9.3	0.1	0.1	0.1

Table 1. Mesh characteristics.

For the closure of turbulence, only eddy-viscosity models have been considered in the present methodology. Other high-order models like the RANS approach (RSM model), or even LES techniques require superior computational requirements and are presumably out of scope for designing purposes. It seems quite convenient the selection of one-equation or, at the most, two-equation models to maintain a low computational cost and speeds up the numerical stage in the design of new prototypes. In particular, this paper shows the results obtained with a one-equation Spalart-Allmaras model (SA) and also with two-equations models including k-ε standard, k-ε RNG and k-ω.

Figure 3 shows the numerical results obtained with the different meshes tested (see table 1) for all the turbulence models considered here. All the results correspond for a flow Reynolds number of $1.4x10^4$.

Whatever turbulence model analyzed, results in figure 3 reveal that differences for the mesh densities are practically negligible, so the sensibility of the numerical model with respect to the spatial discretization is barely relevant. Therefore, the coarser mesh M1 has been finally adopted for the rest of the numerical simulations.

Differences seem to be more significant due to the selection of a particular turbulence model. For both central and lateral holes, the standard k-ε and k-ω models present worse performance than k−ε RNG or SA models, so the latter can be considered as more accurate. Between them, the difference in the lateral holes is quite reduced, but in the central hole, the agreement of the SA results with respect to the experimental data is higher. In summary, the SA model has been selected as an ideal option, due to its accurate agreement and the simplicity of its turbulence closure (just one-equation, originally conceived for aeronautical applications).

In the next section, the distributions of the pressure coefficient, the calibration coefficients and the uncertainty of the measuring system are presented, using the mesh density M1 with a SA turbulence model over a 60 degree trapezoidal THP probe. For every Reynolds number, approximately 20 hours of CPU time were necessary in an Intel(R) dual core 2.5GHz to obtain the variation of the pressure coefficients as a function of the flow angle, from -120 deg to 120 deg at small intervals of 2.5 deg.

RESULTS

Figure 4 shows the results obtained with the numerical simulation for all the pressure coefficients f_i of the trapezoidal THP probe, corresponding to a flow Reynolds number of $1.4x10^4$. The experimental data has been also included in the figure for completeness.

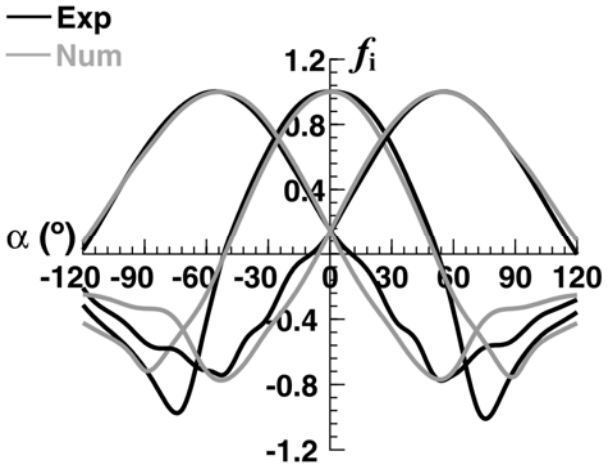

Figure 4. Pressure coefficients, experimental and numerical. Re = 1.4 x 10^4.

Experimentally, it is observed that the distributions of the pressure coefficient in the lateral holes are significantly different from those in the central hole. Moreover, unlike spherical or cylindrical probes, trapezoidal geometries experience minimum values for the central hole in a location

that does not match with the position of the maxima for the lateral holes (around ± 55 deg).

Generally speaking, the numerical model reproduces in a quite reasonable fashion the experimental behavior characteristic of the probe. Major differences arise in very localised positions, associated to partial (or even total) detached conditions of the flow. Thus, some differences are noticeable in the left hole between 0 and +30 deg, as well as in the right hole between 0 and -30 deg, due to the partial detachment of the flow there (small disturbances in the distributions of the pressure coefficients), induced by the sharp edges of the head geometry. Similar behavior is reproduced for the total separation of the flow, that is, from ± 30 deg on (the flow is basically aligned with one of the lateral faces in the probe). In that zone, the experimental values of the pressure coefficients are lower than the numerical results.

In any case, it must be pointed out that the final goal is not the development of a numerical model with extremely high accuracy, allowing a very precise description of the aerodynamical flow behavior, but to provide a general idea (trend) of the probe performance. Notice that an increase of the spatial discretization or the update of the turbulence model (into a higher order for example) may help to put closer both experimental and numerical data, though shooting up the computational cost dramatically. Therefore, the proposed methodology is based on a fast (systematic) numerical characterization of the probe performance that allows the determination of a prototype to be built and tested in a calibration facility experimentally. The results shown in figure 4 confirm the validity of the CFD computations to reduce the overall time of the design process.

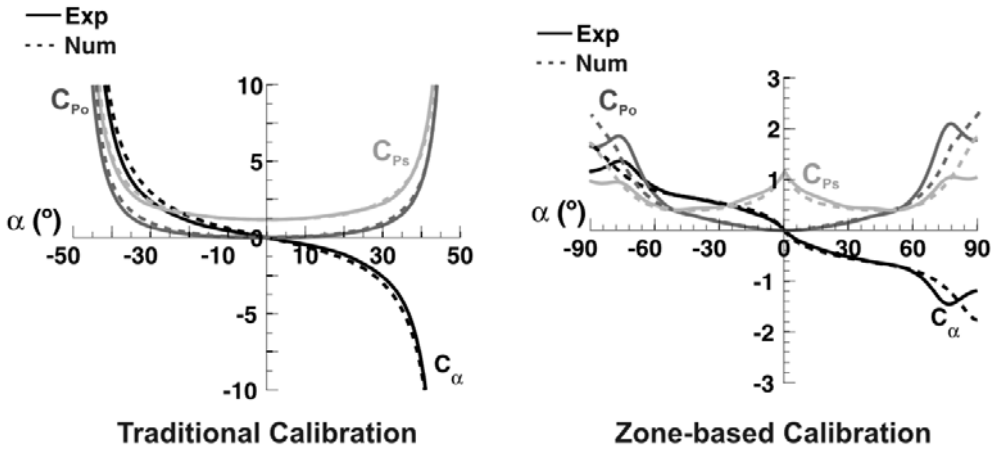

Figure 5. Calibration coefficients, traditional and zone-based, experimental and numerical. Re = 1.4 x 10^4.

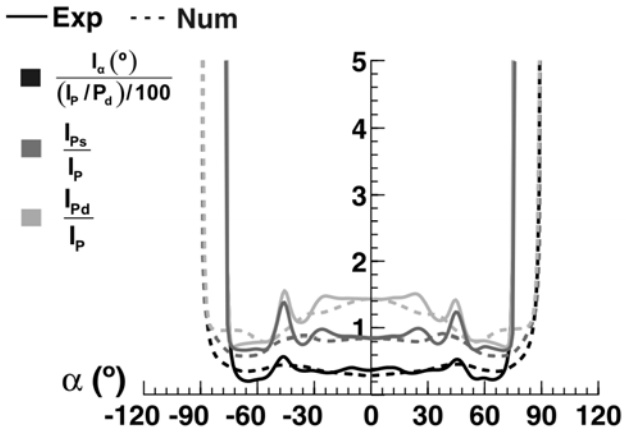

Figure 6. Angle, static pressure and dynamic pressure uncertainty, experimental and numerical. Re = 1.4 x 10^4.

The validity of the numerical model is also confirmed by the results shown in figure 5. Once again, numerical and experimental results are compared, in this case by means of the calibration coefficients. On the left, the traditional definition of the calibration coefficients was employed (equations 1); on the right, equations 2 and 3 corresponding to a two zone-based method were used to represent such calibration coefficients.

In both cases, differences between experimental and numerical data are only appreciable beyond higher flow angles where the flow is fully detached (notice that for the zone-based method this occurs from ± 60 deg on). For lower flow angles the differences are negligible.

The uncertainty transmitted to the retrieved flow variables from the sensors is presented in figure 6. In particular, the uncertainty for the flow angle and both static and dynamic pressures are drawn for a Reynolds number of $1.4x10^4$ as usual, using the classical method proposed by Kline and McClintock [15].

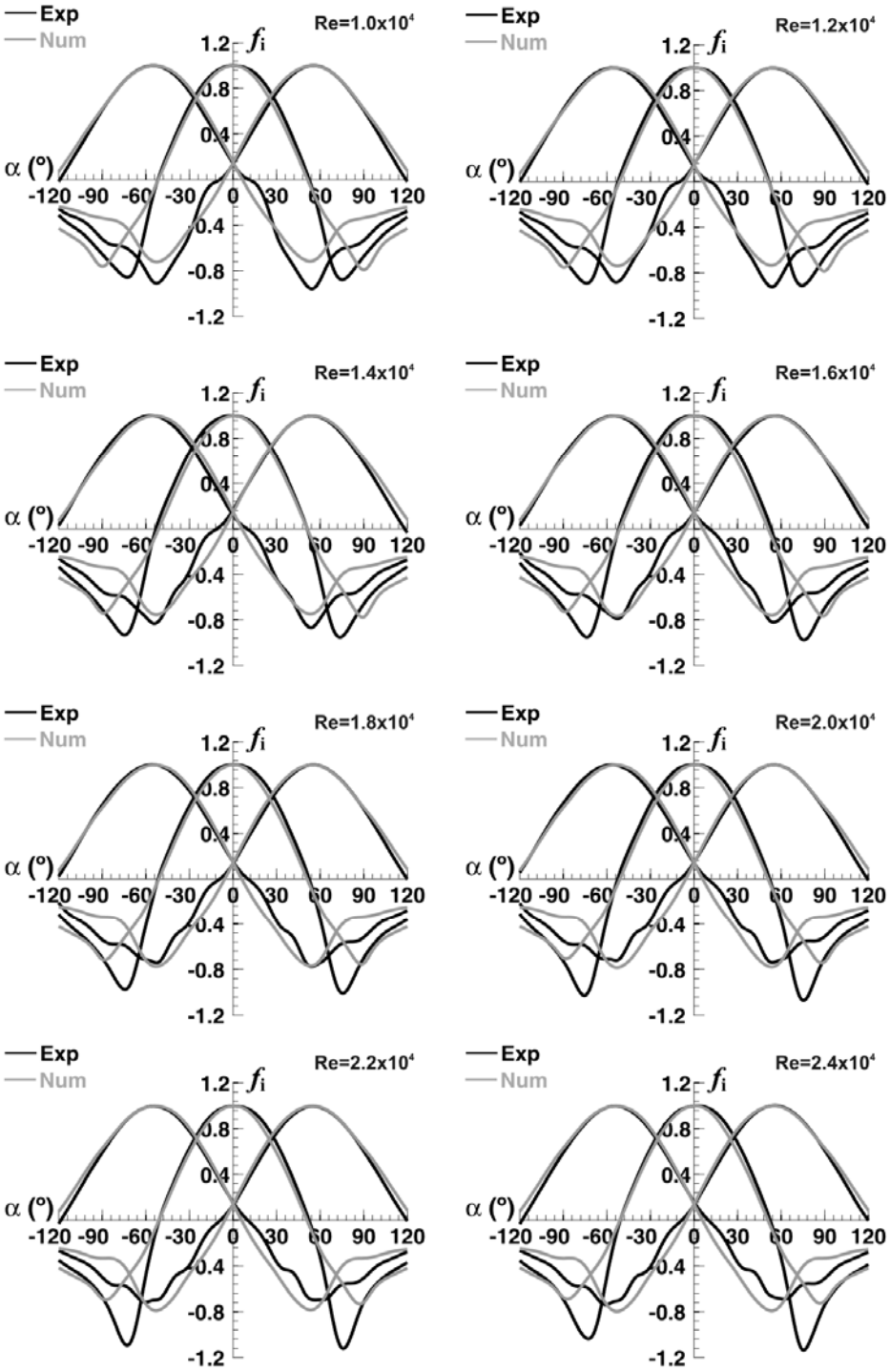

Figure 7. Pressure coefficients for different Reynolds numbers, experimental and numerical.

As exposed in [10], the uncertainty transmitted to the retrieved flow variables is independent of the data reduction technique employed, being exclusively a function of the probe geometry. The uncertainty for the flow angle, I_α (in degrees), is expressed as a percentage of the uncertainty in the pressure measurement I_P, made non-dimensional by the dynamic pressure. The uncertainty of both static and dynamic pressures is adimensionalized with the value of the uncertainty for the pressure measurement.

Experimentally, it is observed that the uncertainty values are quite uniform in the central regions of the angular range, that is, in case of flow angles between ± 30 deg. On the contrary, the uncertainty increases in the external zones of the angular ranges, when the flow separation is set off.

In general, the numerical simulation provides uncertainty levels slightly lower than those obtained in the calibration data, being more evident for the dynamic pressure. However, the overall agreement is reasonable once again, pointing out that the numerical simulation, despite of underpredicting the flow separation in the lateral faces, reproduces quite well the behavior of the uncertainty transmitted to the retrieved flow variables.

The pressure coefficients in THP probes are exclusively a function of the flow angle, being independent of the velocity magnitude, only for a short range of Reynolds numbers. An excellent review describing the effect of the Reynolds number variation over the calibration of five-hole pressure probes can be found in [16].

To determine the sensibility of the numerical model to variations in the velocity of the incident flow, a set of additional simulations was carried out, including the analysis of the probe performance for eight different Reynolds numbers, ranging from $1.0x10^4$ to $2.4x10^4$. Figure 7 shows the pressure coefficients in the holes obtained for every case and compared to the calibration data. Experimentally, it is observed that for flow angles ranging from -30 deg to 30 deg, the pressure coefficients are practically independent of the velocity magnitude, being this effect much more evident for those regions where the flow is detached. It is also observed an inverse trend between the central and lateral holes: in the central orifice, the minimum value of the pressure coefficient is reduced when the Reynolds numbers are high, while being increased for the lateral holes. Since the only significant differences are those where the flow is detached, the numerical model is capturing with a lower precision the effect of the Reynolds number in the distributions of the pressure coefficient.

This is confirmed in the results shown in figure 8, where the effect of the variation in the Reynolds number is observed over the angular calibration coefficient, obtained from a two zone-based method, either experimentally or numerically. Basically, the effects of the velocity magnitude on the angular calibration coefficient are small, with only representative differences for flow angles beyond ±70 deg. This restriction is almost negligible for the numerical simulations resolved here.

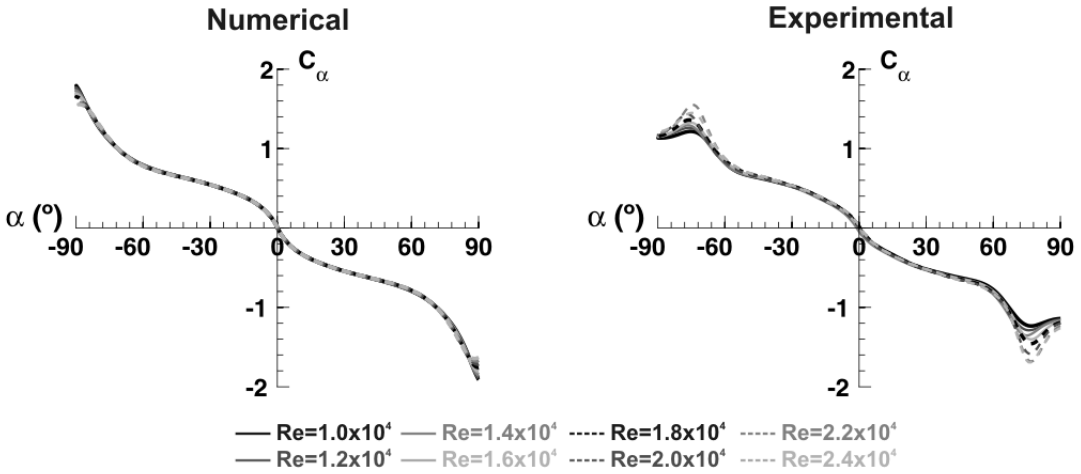

Figure 8. Reynolds number effects on the angular calibration coefficient (zone-based method).

CONCLUSIONS

In this paper a CFD numerical model has been implemented, using the commercial code FLUENT, to simulate the behavior of the incident flow over the holes of THP probes.

The model has been used for a trapezoidal probe, with a separation angle of 60 deg between the holes, to compare these numerical results with experimental data obtained for the probe in a calibration facility.

An analysis of the sensibility of the numerical results to the mesh density has allowed the selection of an optimal mesh in both terms of acceptable accuracy and minimum computational cost. In addition, the selection of simplified geometries and progressive meshes, easy to generate, have permitted the use of systematic strategies for the initial stages of the designing process.

On the other hand, the influence of the turbulence model for the closure of the Navier-Stokes equations has been also explored. It was concluded that the one-equation Spalart-Allmaras model reproduces with reasonable accuracy the

basic features of the probe performance, while maintaining a low computational cost.

The comparison between numerical and experimental results has revealed that the implemented numerical model predicts with sufficient fidelity the basic flow structures around the probe. Major discrepancies appear in those regions affected by flow separation. A precise description of these phenomena would require high-dense meshes and superior turbulence schemes, out of scope of the present methodology.

However, the numerical model presented here is a reliable model, with a relatively low computational cost, that can be employed as a useful tool during the design process of specific pressure probes. With this strategy, prototyping and testing stages can be optimized in order to obtain a definitive probe design with minimum time delays and reduced manufacturing resources.

NOMENCLATURE

CFD	Computational Fluid Dynamics
RNG	Re-Normalization Group
SA	Spallart-Allmaras
THP	Three-Hole Probe
C_α	Angular coefficient
C_{Po}	Total pressure coefficient
C_{Ps}	Static pressure coefficient
f_i	Pressure coefficient
I_α	Angle uncertainty, [deg]
I_P	Pressure uncertainty, [Pa]
I_{Pd}	Dynamic pressure uncertainty, [Pa]
I_{Ps}	Static pressure uncertainty, [Pa]
P_i	Pressure measurement, [Pa]
P_d	Dynamic pressure, [Pa]
P_s	Static pressure, [Pa]
P_0	Total pressure, [Pa]
Re	Reynolds number

Greek Letters

α	Flow angle (yaw angle), [deg]
β	Flow angle (pitch angle), [deg]
δ	Construction angle of the probe, [deg]

REFERENCES

[1] Bryer, D.W. and Pankhurst, R.C., 1974, "Pressure-probe methods for determining wind speed and flow direction", National Physical Laboratory, Her Majesty's Stationary Office, England.

[2] Chue, S.H., 1975, "Pressure probes for fluid measurement", Progress in Aerospace Sciences, **16 (2)**, pp. 147-223.

[3] Dudzinisky, T.J., and Krause, L.N., 1969, ''Flow-direction measurement with fixed-position probes'', NASA TM X-1904.

[4] Lewis, W.E., 1966, ''Fixed-direction probes for aerodynamic measurements'', Proc. Inst. Mech. Eng., **180**, pp. 141-152.

[5] Treaster, A.L. and Yocum A.M., 1979, "The calibration and application of five-hole probes", ISA Transactions, **18**, pp. 23-34.

[6] Sumner, D., 2002, "A comparison of data-reduction methods for a seven-hole probe", ASME Journal of Fluids Engineering, **124**, pp. 523-527.

[7] Ligrani, P.M., Singer, B.A. and Braum, L.R., 1989, "Miniature five-hole pressure probe for measurement of three mean velocity components in low-speed flows", J. Phys. E: Sci. Instrum., **22**. pp. 868-876.

[8] Hooper, J.D. and Musgrove, A.R., 1997, "Reynolds stress, mean velocity and dynamic static pressure measurement by a four-hole pressure probe", Experimental Thermal and Fluid Science, **15**, 375-383.

[9] Kupferschmied, P., Köppel, P., Gizzi, W., Roduner, C. and Gyarmathy, G., 2000, "Time-resolved flow measurements with fast-response aerodynamic probes un turbomachines", Meas. Sci. Technol., **11**, pp. 1036-1054.

[10] Argüelles Díaz, K.M., Fernández Oro, J.M. and Blanco Marigorta, E., 2008, "Direct calibration framework of triple-hole pressure probes for incompressible flow", Meas. Sci. Technol., **19**, pp. 075401.

[11] Argüelles Díaz, K.M., Fernández Oro, J.M. and Blanco Marigorta, E., 2009, "Cylindrical three-hole pressure probe calibration for large angular range", Flow Measurement and Instrumentation, **20**, pp. 57-68.

[12] Argüelles Díaz, K.M., Fernández Oro, J.M. and Blanco Marigorta, E., 2008, "Extended angular range of a three-hole cobra pressure probe for incompressible flow", Journal of Fluids Engineering, **130**, pp. 101401.

[13] Argüelles Díaz, K. M., Fernández Oro, J.M. and Blanco Marigorta, E., 2008, "Three-hole pressure probes at large", XIX Biannual Symposium on Measuring Techniques in Turbomachinery. Transonic and Supersonic Flow in Cascades and Turbomachines (Belgium).

[14] Smout, P.D. and Ivey, P.C., 1997, "Investigation of wedge probe wall proximity effects: part 2 – numerical and analytical modelling", ASME Journal of Engineering for Gas Turbines and Power, **119**, pp. 605-611.

[15] Kline, S.J. and McClintock, F.A., 1953, "Describing uncertainties in single sample experiments", Mech. Eng. (Am. Soc. Mech. Eng.), **75**, pp. 3-8.

[16] Dominy, R.G. and Hodson, H.P., 1993, "An investigation of factors influencing the calibration of five-hole probes for three-dimensional flow measurements", Journal of Turbomachinery, **115**, pp. 513-519.